

Title	Practical procedure for retrieval of quantitative phase map for two-phase interface using the transport of intensity equation
Author(s)	Zhang, Xiaobin; Oshima, Yoshifumi
Citation	Ultramicroscopy, 158: 49-55
Issue Date	2015-07-04
Type	Journal Article
Text version	author
URL	http://hdl.handle.net/10119/15374
Rights	Copyright (C)2015, Elsevier. Licensed under the Creative Commons Attribution-NonCommercial-NoDerivatives 4.0 International license (CC BY-NC-ND 4.0). [http://creativecommons.org/licenses/by-nc-nd/4.0/] NOTICE: This is the author's version of a work accepted for publication by Elsevier. Xiaobin Zhang, Yoshifumi Oshima, Ultramicroscopy, 158, 2015, 49-55, http://dx.doi.org/10.1016/j.ultramic.2015.06.015
Description	

Practical procedure for retrieval of quantitative phase map for two-phase interface using the transport of intensity equation

Xiaobin Zhang^{1,2}, Yoshifumi Oshima^{2,3}

¹Quantum Nanoelectronics Research Centre, Tokyo Institute of Technology,
2-12-1-H-51 Oh-okayama, Meguro-ku, Tokyo 152-8551, Japan

²CREST, JST

³School of Materials Science, JAIST, 1-1 Asahidai, Nomi, 923-1292, Japan

E-mail : zhang.x.am@m.titech.ac.jp

Abstract

A practical procedure for retrieving quantitative phase distribution at the interface between a thin amorphous germanium (a-Ge) film and vacuum based on the transport of intensity equation is proposed. First, small regions were selected in transmission electron microscopy (TEM) images with three different focus settings in order to avoid phase modulation due to low frequency noise. Second, the selected TEM image and its three reflected images were combined for mirror-symmetry to meet the boundary requirements. However, in this symmetrization, extra phase modulation arose due to the discontinuous nature of Fresnel fringes at the boundaries among the four parts of the combined image. Third, a corrected phase map was obtained by subtracting a linear fit to the extra phase modulation. The phase shift for a thin a-Ge film was determined to be approximately 0.5 rad, indicating that the average inner potential was 18.3 V. The validity of the present phase retrieval is discussed using simple simulations.

Key words: Transport of intensity equation; TEM; Phase map

1. Introduction

The potential distribution at two-phase interfaces is important for understanding the physical and chemical properties of devices. Recently, the local potential distribution at the interface between cathode (anode) materials and an electrolyte has been a key issue for improvements of lithium-ion batteries [1,2] since battery performance is related to local lithium diffusion at the interface, which depends on the local potential.

Transmission electron microscopy (TEM) is a powerful tool for determining not only the local structure, but also the local potential distribution, since the phase shift of the incident electron wave is proportional to the local potential. The phase shift can be measured using methods such as electron holography (EH) [3], focal series reconstruction methods [4], diffractive imaging [5] and the transport of intensity equation (TIE) [6-13]. Among these, EH, which reconstructs the phase using the interference between an object wave that passes through the specimen and a reference wave that passes through vacuum, is the most popular method. However, installation of a biprism into the TEM column is necessary in order to deal with interference, and a vacuum region for the reference wave is also essential. These requirements restrict the application of EH.

Phase information can also be retrieved by utilizing the principle of wave propagation, and the TIE is one such approach [6-13]. The TIE does not require any special microscope attachments or a vacuum region, and is thus considered to have a wider scope for applications compared to EH. The TIE has been used to determine the mean inner potential (MIP) of metallic nanoparticles [14-16], and it was found that the MIP increases as the particle diameter decreases to a few nanometers. Petersen et al. investigated the quantitative TIE-retrieved phase energetically from various aspects including precise determination of the defocus value and estimation of the modulation transfer function for a charge-coupled device (CCD) detector [17]. They also demonstrated a quantitative TIE-retrieved phase map for MgO nanocubes [18]. The TIE has also been used to observe helical spin order [19] and two-dimensional skyrmion crystal phases [20,21].

However, the phase distribution at the interface has been rarely investigated using the TIE method thus far. One of the reasons is the requirement of boundary conditions. The Fresnel fringes of an object, which contains the phase information, vary with defocus in a TEM image, and should not spread to the outside of the image area in order for phase retrieval. In the case of metallic nanoparticles adsorbed on a uniform substrate, a suitable region surrounding the nanoparticle can be selected to contain all Fresnel

fringes of the particle. However, as for an interface, the Fresnel fringes in the vicinity of the interface are subject to be cut off by selecting a region, which causes artifact in the retrieved phase. This is because the discontinuous Fresnel fringes at the boundary are assumed to be periodic and continually connected with each other when carrying out Fourier transform (FFT) calculation. Volkov et al. proposed a mirror-symmetrization method to solve such problem [10]. If the original TEM image meet the intensity conservation law, which means the total intensity is maintained regardless of defocus, then the phase shift at the interface can be correctly retrieved. This has been demonstrated effective through simulation in their article.

Low-frequency noise has been shown to be amplified, which is also a problem for quantitative phase retrieval [11,17,22,23]. The phase change at a two-phase interface has been reconstructed by employing an image mask for noise subtraction [23]. However, these methods do not seem to be sufficiently practical.

In this study, we demonstrated that the phase distribution can be quantitatively retrieved for the interface between a thin amorphous germanium (a-Ge) film and vacuum using the TIE-FFT method. Using a selection of small regions in the TEM images was effective at removing low-frequency noise. In addition, mirror-symmetrization of the experimental TEM image and subtraction of the linear background was found to be necessary.

2. Experimental methods

TEM observations were conducted using a 50 pm resolution electron microscope (R005) equipped with a cold field emission gun and double spherical aberration-correctors, operated at an accelerating voltage of 300 kV [24]. In this study, TEM images were obtained with a spatial resolution of 0.84 nm/pixel. A through-focus image series was obtained from -10 μm (under-focus) to +10 μm (over-focus) in steps of 2 μm by changing the objective lens current. Under-focus usually has minus sign in this study. Aberration of the imaging lens was corrected below the fourth-order and the chromatic aberration was 1.65 mm. The TIE phase retrieval procedure was performed using the QPt (HREM Research Inc.) plug-in software [25] for Digital Micrograph (Gatan Inc.). In this procedure, three TEM images (under-, in- and over-focus) were aligned at the sub-pixel level.

For the analysis, the MIP was calculated using

$$\varphi(x) = C_E V_0 t(x), \quad (1)$$

where C_E is a constant that is related to the electron energy ($C_E = 6.523 \times 10^{-6}$ rad V^{-1} nm^{-1} at an acceleration voltage of 300 kV), V_0 is the MIP (assuming that the MIP is constant) and $t(x)$ is the thickness distribution. Using Eq. (1), V_0 could be calculated when $t(x)$ and the phase shift $\varphi(x)$ were experimentally obtained.

The thin a-Ge film used in this study was a commercial product. As a simple case, the film/vacuum interface was considered to be better than a solid/solid interface to clarify the problem that whether the potential distribution at the interface could be estimated quantitatively by TIE method. The present phase retrieval method is also thought to be useful for a solid/solid interface under certain conditions.

For TEM observations, the current density needs to be as low as possible in order to suppress irradiation damage; however a certain amount of current density is necessary in order to improve the signal-to-noise ratio. Therefore, the optimal current density was determined by the balance between these two requirements.

The thickness of the thin a-Ge film was estimated from electron energy-loss spectroscopy (EELS) measurements. The EELS spectrum was obtained with an aperture size of 54 mrad, an exposure time of 0.05 s and an energy dispersion of 0.1 eV/channel. The inelastic mean free path λ , was calculated to be 153 nm using the expression given in Ref. [26]. The thickness was determined by multiplying the inelastic mean free path and the logarithm of the ratio of the total area to the zero-loss area.

3. Experimental Results

A typical TEM image at the edge of the thin a-Ge film is shown in Fig. 1. The left side is the vacuum region and the right side is the film. In the three TEM images with different focuses (-8, 0 and +8 μm), four small regions as indicated by the squares in Fig. 1 (ca. 41×41 nm^2) were selected and mirror-symmetrized accordingly. The original images were rotated to the right by 45° before mirror-symmetrization. Figs. 2(a-c) show the mirror-symmetrized results for three different focuses of area in Fig. 1(d). In the mirror-symmetrized image, the thin a-Ge film is surrounded by vacuum regions on all sides, which have constant intensity regardless of defocus. By applying the TIE method to these TEM images, the phase map could be retrieved as shown in Fig. 2(d). In the map, the brighter and darker regions correspond to the thin a-Ge film and the vacuum, respectively, indicating that the phase map seemed to be retrieved correctly to some extent.

Figure 3 shows TIE-retrieved phase maps of four selected regions indicated by (a) to (d) in Fig. 1. The selection and symmetrization of these small regions in the TEM image

enabled a phase map of the interface to be reproducibly retrieved. However, the obtained (raw) phase maps (left column of Fig. 3) were unexpectedly modulated at the vacuum region. We considered that this might be caused by the discontinuity of the Fresnel fringes at the boundaries among the four parts of the mirror-symmetrized TEM image. Thus, in order to obtain a corrected phase map, the phase modulations in vacuum need to be subtracted as a non-physical quantity from the raw phase maps.

The phase profile perpendicular to the interface in the raw phase maps had a tendency to increase gradually even at the vacuum region and the thin a-Ge film region, as shown in Fig. 4(a), although it should be constant. The phase profiles perpendicular to the interface were investigated line-by-line in the four phase maps in the left column of Fig. 3. We found that the profiles could be approximated by a straight line at the vacuum region, although their gradients were different from line to line. Therefore, a linear fit was obtained in the vacuum region using the least squares method, and was then extrapolated toward the thin film, as shown by dotted line in Fig. 4(a). A quadratic background did not provide a suitable fit for the phase profile. Each corrected phase profile was obtained line-by-line by subtracting the linear fit from the raw phase profile, and the corrected two-dimensional phase map was composed by these corrected one-dimensional phase profiles. The corrected phase maps in the right column of Fig. 3 seem reasonable, since the phases are almost constant in both the vacuum and thin a-Ge film regions.

Figure 4(b) shows phase profiles along the diagonals of the four corrected phase maps. The phase profiles are similar to each other, indicating that the phase maps are reproducibly obtained. The phase shift was determined to be approximately 0.5 rad at the interface. No dip or spike appears at the interface, which suggests that the inner potential or/and thickness must change gradually at the interface between the a-Ge film and vacuum.

The thickness of the thin a-Ge film was determined by EELS measurement. The logarithm of the ratio of the total area to the zero-loss area was 0.025 to 0.03, so that the film thickness was determined to be 4.2 ± 0.4 nm. The error may come from several factors. First, the log ratio method estimates the specimen thickness only roughly, because inelastic electron scattering is a probabilistic phenomenon and its spectrum has a certain background noise. Second, the thickness of the thin a-Ge film is not absolutely uniform. This resulted in variation in the estimated thickness. Therefore, the inner potential was determined to be 18.3 ± 1.8 V, which is higher than that reported for a Ge crystal (theoretical value of 14.7 V [27] and experimental value of 14.3 V [28]). The apparent inner potential has been reported to increase with decreasing specimen

thickness due to surface tension [29]. Taking into account the fact that the observed a-Ge film was very thin, this high potential may be partially caused by a surface-related electrostatic potential.

To investigate the dependence of the TIE-retrieved phase map on the TEM image size, square regions with side lengths of 161, 120 and 41 nm were selected from the experimental TEM image (Fig. 5(a)). After mirror-symmetrization as Fig. 5(b), the TIE phase maps were obtained (Fig. 5(c)). In the cases of the 161×161 and 120×120 nm² regions, unexpected phase patterns covered the entire area of the phase map. However, in the case of the 41×41 nm² region, these patterns were suppressed. This indicates that the low frequency components, which were amplified in the TIE-retrieved phase map, were removed by small region selection.

4. Discussion

We have shown that the phase map at the interface between a thin a-Ge film and a vacuum region can be reproducibly obtained by using a small region, mirror-symmetrization and subtraction of the non-physical phase distribution.

The relationship between the noise level and phase modulation was first investigated. In the vacuum region of the TEM image, the intensity histogram could be approximated by a Gaussian distribution with a deviation of 0.03 (Fig. 6(a)). Such an intensity distribution can be explained by statistical error. By creating TEM images that have white noise with a deviation of 0.03, phase modulations were obtained for the 161×161, 120×120 and 41×41 nm² regions, as shown in Fig. 6(b). We found that the amount of phase modulation decreased with the size of the selected region. For the 41×41 nm² region, the phase value varied within the range 0 to 0.17 rad when the phase shift for the a-Ge film was 0.5 rad. The phase modulation due to low-frequency noise was lower than the phase shift of the interface, indicating that the selected 41×41 nm² region is sufficiently small to retrieve the phase map for the interface.

Next, the validity of the procedure to obtain a corrected phase map is discussed. For the simulation, an amorphous carbon (a-C) structure consisting of 1720 carbon atoms in a 2.13×2.13×2.13 nm³ cubic cell was simulated using molecular dynamics calculations. The projected potential map for the a-C structure is shown in Fig. 7(a) as a reference. Figure 7(b) shows the phase map, which corresponds to the square region outlined in Fig. 7(a) in the phase map (not shown) retrieved from the three simulated TEM images with different focus conditions (-20, 0 and +20 nm). This phase map was correctly retrieved, since the a-C structure was surrounded by the vacuum region in the simulated

TEM images. Thus, the phase map in Fig. 7(b) reproduces the projected potential map in Fig. 7(a) well, except for a reduction in the spatial resolution. The phase shift at the vacuum region is almost zero, while that at the interface is approximately 0.3 rad, which is almost the same as that for the projected potential.

The TIE-retrieved phase at the interface between the a-C structure and vacuum regions was also obtained from a mirror-symmetrized TEM image (Fig. 7(c)) and from a mirror-symmetrized TEM image with white noise (Fig. 7(d)). Same regions in the simulated TEM images with Fig. 7(b) were used for mirror-symmetrization. In both phase maps, non-physical phase modulation appears in the vacuum region. In Fig. 7(d), this can be explained by low-frequency noise as mentioned above, whereas in Fig. 7(c), it cannot be explained by noise, because it is noiseless.

In order to understand the reason for such non-physical phase modulation, we investigated the relationship between the discontinuity of Fresnel fringes at the boundaries among the four parts of the mirror-symmetrized TEM image and the phase modulation. In the simulation results (see supplementary data), non-physical phase modulation which looks like a rounded quadrangular pyramid, arose due to the discontinuity of Fresnel fringes at the boundaries. The real phase map can be obtained by subtracting such modulations from the original phase map.

The original phase profiles along the diagonal of three TIE-retrieved phase maps (Fig. 7(b–d)) are shown in Fig. 7(e). By subtracting the linear background profiles from the original ones, the corrected phase profiles correspond to phase maps in Fig. 7(c) and (d) were obtained as shown in Fig. 7(f). These profiles are in agreement with that of Fig. 7(b), which is the evidence of that subtraction of the linear background is a reasonable approach to obtain a corrected phase map of the interface.

In the present study, we investigated the simple case of the thin a-Ge film/vacuum interface in order to propose a practical procedure for phase retrieval using TIE method. The present procedure can also be applied to a solid/solid interface, when the inner potential and thickness are constant in both solid regions.

5. Summary

We have demonstrated that the phase distribution at the interface between a thin a-Ge film and a vacuum region can be reproducibly retrieved by solving the TIE using FFT. The selection of small regions in the TEM images was effective to avoid phase modulation caused by low-frequency noise. In addition, mirror-symmetrization of the TEM images is necessary to satisfy the intensity conservation law. However, these two

procedures are not sufficient to obtain a quantitative phase map at the interface, because non-physical phase modulation remained due to the discontinuity of Fresnel fringes at the boundaries among the four parts of the mirror-symmetrized TEM images. The non-physical phase profile perpendicular to the interface could be approximated by linear fitting in the vacuum region and by extrapolation toward the thin film. A corrected phase map was then reproducibly obtained by subtracting the linear fit from the original TIE-retrieved phase profile line-by-line. The retrieved phase shift for the thin a-Ge film was determined to be approximately 0.5 rad, which indicates that the average inner potential was 18.3 V. This value is slightly higher than that previously reported [31], which could be explained by a surface-related electrostatic potential. The procedures outlined here are sufficiently practical to obtain a quantitative phase map of two-phase (solid/solid) interfaces.

Acknowledgements

The authors thank Prof. Takayanagi, Dr. Mitome and Dr. Ishizuka for constructive comments and fruitful discussions. This work was supported by the Japan Science and Technology Agency (JST) under the CREST project.

References

- [1] K. Yamamoto, Y. Iriyama, T. Asaka, T. Hirayama, H. Fujita, C. A. J. Fisher, K. Nonaka, Y. Sugita, Z. Ogumi, Dynamic Visualization of the Electric Potential in an All-Solid-State Rechargeable Lithium Battery, *Angew. Chem.* 122 (2010) 4516–4519.
- [2] K. Yamamoto, Y. Iriyama, T. Asaka, T. Hirayama, H. Fujita, K. Nonaka, K. Miyahara, Y. Sugita, Z. Ogumi, Direct observation of lithium-ion movement around an in-situ-formed-negative-electrode/solid-state-electrolyte interface during initial charge–discharge reaction, *Electrochem. Commun.* 20 (2012) 113–116.
- [3] A. Tonomura, N. Osakabe, T. Matsuda, T. Kawasaki, J. Endo, S. Yano, H. Yamada, Evidence for Aharonov-Bohm effect with magnetic field completely shielded from electron wave, *Phys. Rev. Lett.* 56 (1986) 792–795.
- [4] L. J. Allen, M. P. Oxley, Phase retrieval from series of images obtained by defocus variation, *Opt. Commun.* 199 (2001) 65–75.
- [5] S. Morishita, J. Yamasaki, K. Nakamura, T. Kato, N. Tanaka, Diffractive imaging of the dumbbell structure in silicon by spherical-aberration-corrected electron diffraction, *Appl. Phys. Lett.* 93 (2008) 183103.

- [6] M. R. Teague, Deterministic phase retrieval: a Green's function solution, *J. Opt. Soc. Am.* 73 (1983) 1434–1441.
- [7] D. Paganin, K. A. Nugent, Noninterferometric Phase Imaging with Partially Coherent Light, *Phys. Rev. Lett.* 80 (1998) 2586–2589.
- [8] M. De Graef, Lorentz Microscopy: Theoretical Basis and Image Simulations, in: M. De Graef, Y. Zhu (Eds), *Magnetic Imaging and Its Applications to Materials*, Academic Press, San Diego, 2001, pp. 27–67.
- [9] M. De Graef, Y. Zhu, Quantitative noninterferometric Lorentz microscopy, *J. Appl. Phys.* 89 (2001) 7177–7179.
- [10] V. V. Volkov, Y. Zhu, M. De Graef, A new symmetrized solution for phase retrieval using the transport of intensity equation, *Micron* 33 (2002) 411–416.
- [11] V. V. Volkov, Y. Zhu, Deterministic phase unwrapping in the presence of noise, *Optics Letters* 28 (2003) 2156–2158.
- [12] D. Paganin, A. Barty, P. J. McMahon, K. A. Nugent, Quantitative phase-amplitude microscopy. III. The effects of noise, *J. Microsc.* 214 (2004) 51–61.
- [13] K. Ishizuka, B. Allman, Phase measurement of atomic resolution image using transport of intensity equation, *J. Electron Microsc.* 54 (2005) 191–197.
- [14] T. C. Petersen, M. Bosman, V. J. Keast, G. R. Anstis, Plasmon resonances and electron phase shifts near Au nanospheres. *Appl. Phys. Lett.* 93 (2008) 101909.
- [15] M. Mitome, K. Ishizuka, Y. Bando (2010) Quantitativeness of phase measurement by transport of intensity equation. *J. Electron Microsc.* **59**: 33–41.
- [16] P. Donnadieu, S. Lazar, G. A. Botton, I. Pignot-Paintrand, M. Reynolds, S. Perez, Seeing structures and measuring properties with transmission electron microscopy images: A simple combination to study size effects in nanoparticle systems, *Appl. Phys. Lett.* 94 (2009) 263116.
- [17] T. C. Petersen, V. J. Keast, K. Johnson, S. Duvall, TEM-based phase retrieval of p–n junction wafers using the transport of intensity equation, *Philos. Mag.* 87 (2007) 3565–3578.
- [18] T. C. Petersen, V. J. Keast, D. M. Paganin, Quantitative TEM-based phase retrieval of MgO nano-cubes using the transport of intensity equation, *Ultramicroscopy* 108 (2008) 805–815.
- [19] M. Uchida, Y. Onose, Y. Matsui, Y. Tokura, Real-Space Observation of Helical Spin Order, *Science* 311 (2006) 359–361.
- [20] X. Yu, N. Kanazawa, Y. Onose, K. Kimoto, W. Z. Zhang, S. Ishiwata, Y. Matsui, Y. Tokura, Near room-temperature formation of a skyrmion crystal in thin-films of

- the helimagnet FeGe. *Nat. Mater.* 10 (2011) 106–109.
- [21] X. Yu, Y. Onose, N. Kanazawa, J. H. Park, J. H. Han, Y. Matsui, N. Nagaosa, Y. Tokura, Real-space observation of a two-dimensional skyrmion crystal, *Nature* 465 (2010) 901–904.
- [22] D. Paganin, A. Barty, P. J. McMahon, K. A. Nugent, Quantitative phase-amplitude microscopy. III. The effects of noise, *J. Microsc.* 214 (2004) 51–61.
- [23] M. Beleggia, M. A. Schofield, V. V. Volkov, Y. Zhu, On the transport of intensity technique for phase retrieval, *Ultramicroscopy* 102 (2004) 37–49.
- [24] H. Sawada, Y. Tanishiro, N. Ohashi, T. Tomita, F. Hosokawa, T. Kaneyama, Y. Kondo, K. Takayanagi, STEM imaging of 47-pm-separated atomic columns by a spherical aberration-corrected electron microscope with a 300-kV cold field emission gun, *J. Electron Microsc.* 58 (2009) 357–361.
- [25] <http://www.hremresearch.com/> HREM Research Inc.
- [26] K. T. Moore, E. A. Stach, J. M. Howe, D. C. Elbert, D. R. Veblen, A tilting procedure to enhance compositional contrast and reduce residual diffraction contrast in energy-filtered TEM imaging of planar interfaces, *Micron* 33 (2002) 39–51.
- [27] P. Kruse, M. Schowalter, D. Lamoen, A. Rosenauer, D. Gerthsen, Determination of the mean inner potential in III–V semiconductors, Si and Ge by density functional theory and electron holography, *Ultramicroscopy* 106 (2006) 105–113.
- [28] J. Li, M. R. McCartney, R. E. Dunin-Borkowski, D. J. Smith Determination of mean inner potential of germanium using off-axis electron holography, *Acta Crystallographica Section A* 55 (1999) 652–658.
- [29] M. Wanner, D. Bach, D. Gerthsen, R. Werner and B. Tesche, Electron holography of thin amorphous carbon films: Measurement of the mean inner potential and a thickness-independent phase shift, *Ultramicroscopy* 106 (2006) 341–345.

Figure caption

Figure 1

A typical TEM image of the interface between a thin a-Ge film and a vacuum taken at under-focus 8 μm . Four TIE-retrieved phase maps were obtained at the small regions denoted by (a–d).

Figure 2

The experimental TEM image indicated by a yellow square (the lowest one) in Fig. 1 and its three reflected images were combined to have mirror-symmetry. (a–c) Typical mirror-symmetrized TEM images of under-, in- and over-focus, respectively. The thin a-Ge films in these images are surrounded by the vacuum regions on all sides. (d) Typical TIE-retrieved phase map obtained from TEM images (a–c). The brighter and darker regions correspond to the thin a-Ge film and the vacuum, respectively.

Figure 3

(a–d) TIE-retrieved phase maps obtained at the small regions denoted by (a–d) in Fig. 1, respectively. The left column shows the original phase maps, while the right column shows the corrected phase maps obtained by subtraction of the linear background from the original ones.

Figure 4

(a) Typical original (solid line), corrected (bold line), and linear background (dashed line) phase profiles. The linear background was determined by fitting the phase modulation at the vacuum region using the least squares method and extrapolation toward the thin film. The corrected phase map was obtained by subtracting the linear background from the original one. (b) Four corrected phase profiles obtained from the four phase maps in the right column of Fig. 3.

Figure 5

(a) Typical TEM image of the interface between the a-Ge film and vacuum region taken at under-focus 8 μm . Three different small regions are indicated by green, yellow and red squares in the TEM image with sizes of 161×161 , 120×120 and 41×41 nm^2 , respectively. (b) Mirror-symmetrized TEM images of the three small regions. The sizes became 322×322 , 241×241 and 83×83 nm^2 , respectively. (c) The corresponding

TIE-retrieved phase maps.

Figure 6

(a) Histogram of image intensity in the vacuum region. The image intensity is normalized. The intensity distribution is well fitted by a Gaussian function with a deviation of 0.03, as indicated by the red curve. (b) TIE-retrieved phase maps for TEM images with white noise and a deviation of 0.03. The sizes are the same as the experimental results shown in Fig. 5. The maximum phase values are 0.59, 0.34 and 0.17 for the maps of the 322×322 , 241×241 and 83×83 nm² regions, respectively.

Figure 7

(a) Projected potential map of the a-C structure obtained by molecular dynamic calculations. The TIE-retrieved phase map was obtained at the square region outlined in yellow. (b) TIE-retrieved phase map for the simulated TEM images of three different defoci: -20, 0 and +20 nm. (c) TIE-retrieved phase map obtained from the mirror-symmetrized TEM image. (d) TIE-retrieved phase map obtained from the mirror-symmetrized TEM image with white noise. (e) Original phase profiles for the non-symmetrized image (solid line), mirror-symmetrized image (dashed line), and mirror-symmetrized image with white noise (bold line). The straight dashed and solid lines correspond to the linear background profiles. (f) Corrected phase profiles for the non-symmetrized image (solid line), mirror-symmetrized image (dashed line), and mirror-symmetrized image with white noise (bold line).

Figures

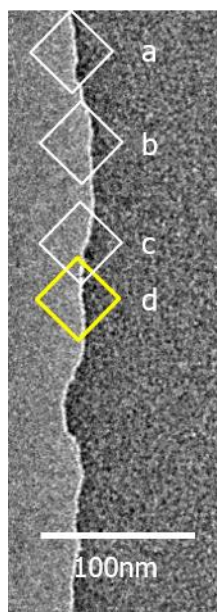


Figure 1

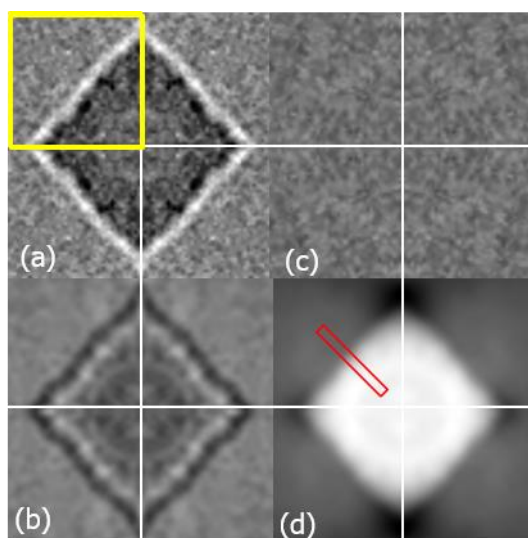


Figure 2

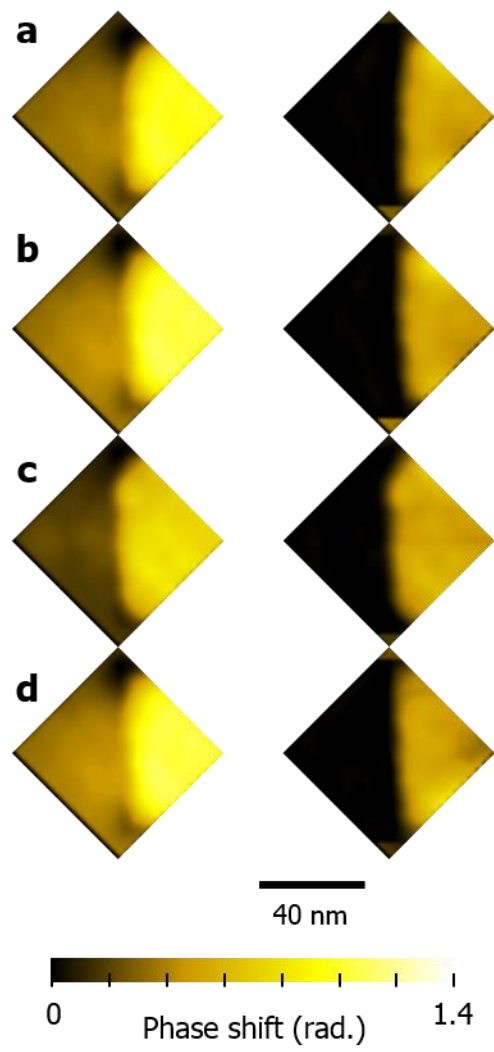


Figure 3

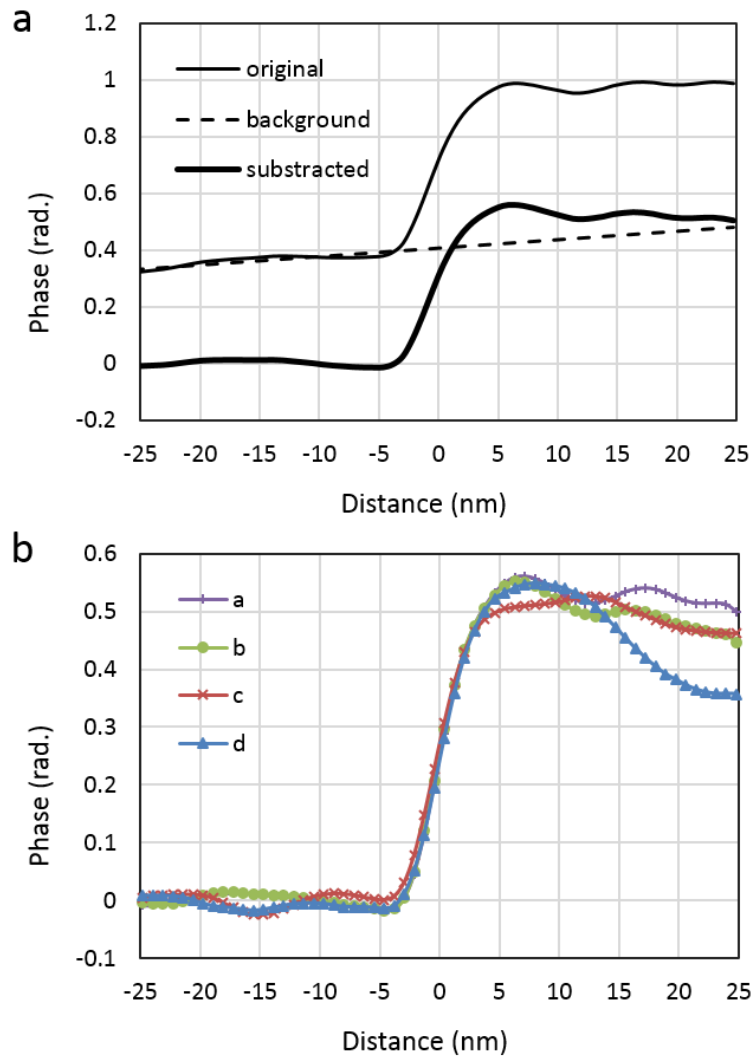


Figure 4

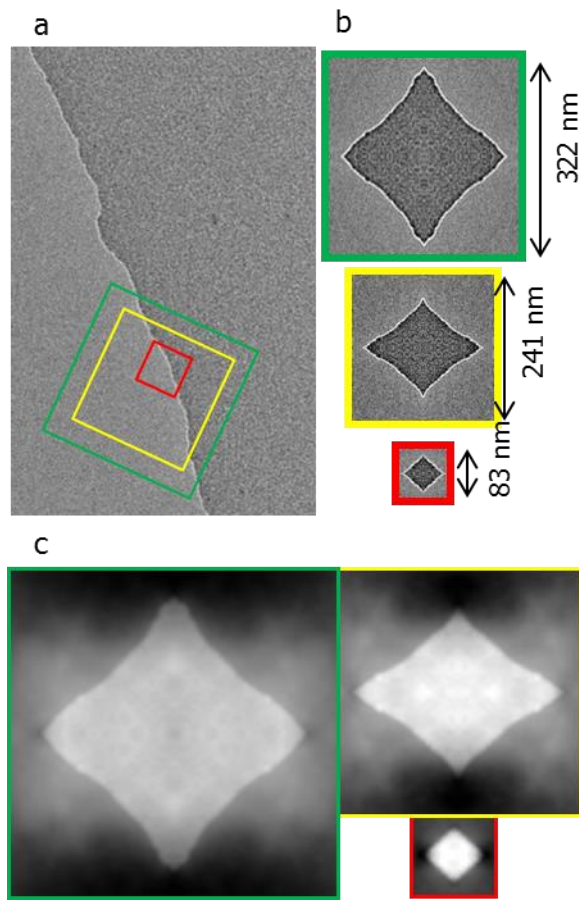


Figure 5

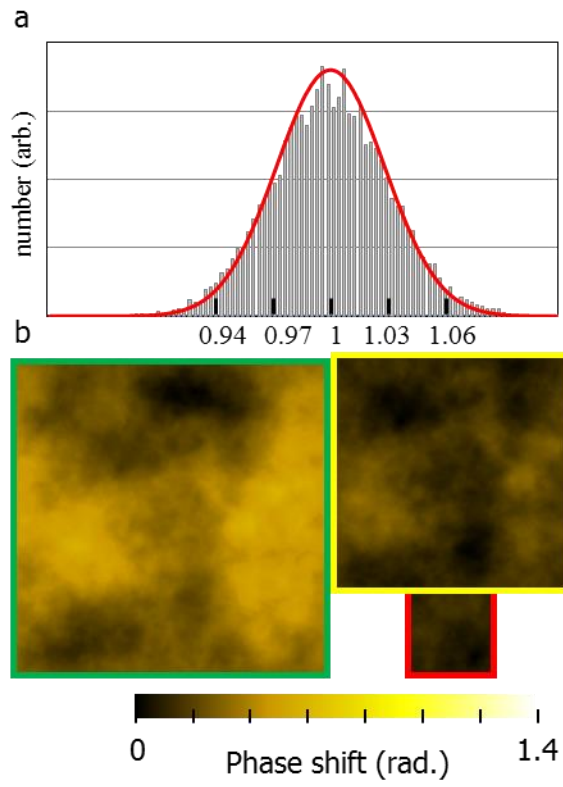


Figure 6

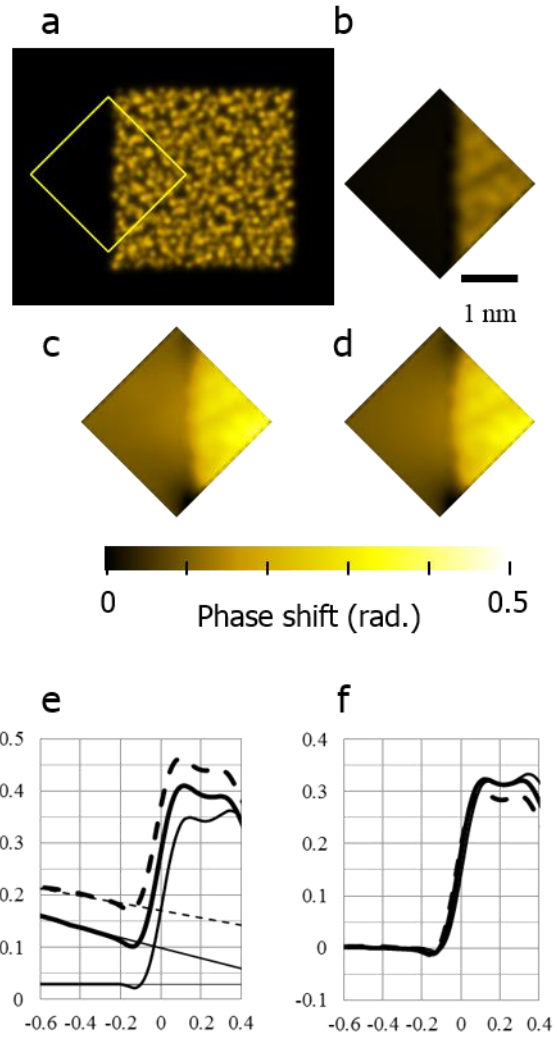


Figure 7